Characteristics of Turbulent Flow in the Annuli with Smooth and Rough Surfaces

Soo Whan Ahn* and Kyung Chun Kim**

(*Received April 8, 1998*)

The structure of turbulence of fully developed flow through three concentric annuli with rough walls shown in Fig. 1 was investigated experimentally for Reynolds number range of Re =15000−66000. Time mean velocity distribution, friction factor, turbulence intensity and turbulent kinetic energy in annuli of three radius ratios of α=0.26, 0.39 and 0.56 for four cases of roughness type were measured. The results show that the structure of turbulence in these asymmetric flows is significantly different depending on the roughness wall position. An experimental study for the case of a smooth annulus was also carried out for a benchmarking purpose. The velocity distributions and friction factors are also presented and discussed.

Key Words: Friction Factor, Turbulence Intensities, Turbulent Kinetic Energy, Concentric Annuli, Wall Roughness

1. Introduction

In non-circular channels of practical importance which have complex boundary conditions, the velocity profiles are asymmetric and the position of zero shear stress is not coincident with that of zero velocity gradient. These asymmetric velocity profiles result from the interaction of two flow zones of different sizes and different kinetic energy of the turbulence field. One of simplest non-circular flow channels is a smooth concentric annulus. The annulus generates an asymmetric velocity profile, which becomes more asymmetric at smaller radius ratio ($\alpha=R_i/R_o$) of the inner and outer radii of the annulus. For this channel, a number of experimental investigations (Brighton & Jones, 1964, Rehme, 1974) were performed on the pressure drop and the velocity distribution. Significant deviations from the behaviour of symmetrical flows were shown, such as the non-coincidence of the position of zero shear stress with that of maximum velocity and a difference from the law of the wall of the dimensionless velocity distribution in the inner zone of annuli. Brighton (1963) and Brighton & Jones (1964) for the first time published the experimental results on turbulence intensities in three directions, and on radial shear stresses in a smooth annuli; four different radius ratios were used by Brighton. Kjellström & Hedberg (1966) and Durst (1968) investigated the turbulence in the same smooth annulus experimentally; but they measured only the turbulence intensities in the axial and radial directions as well as the radial shear stresses. Lawn & Elliot (1971) published the results of turbulence measurements in smooth annuli with three different radius ratios. Both Brighton's (1963) and Lawn & Elliot's (1971) investigations used fairly small radius ratios (α=0.0625 and 0.088, respectively) and they observed highly asymmetric velocity distributions, whereas Kjellström & Hedberg (1966) and Durst (1968) used a radius ratio of α=0.446, for which the velocity distribution was only slightly asymmetric, however, thus not relevant to asymmetric velocity distributions. But since Brighton (1963) and Lawn & Elliot (1971) used spacers to fix the core tubes, the spacers may

* Department of Marine Engineering, Gyeongsang National University, Institute of Marine Industry, Tongyong Kyongnam, 650-160, Korea

** School of Mechanical Engineering, Pusan National University. Research Institute of mechanical Technology, Jangjun-Dong, Kumjung-Gu, Pusan, 609-735, Korea

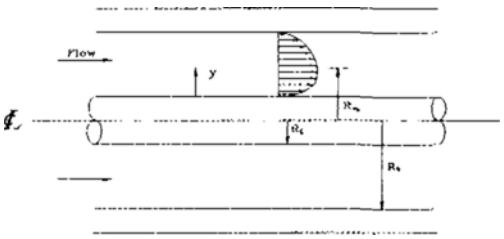

(a) Case

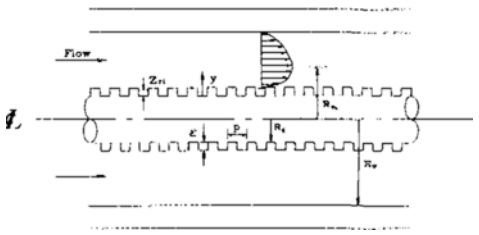

(b) Case

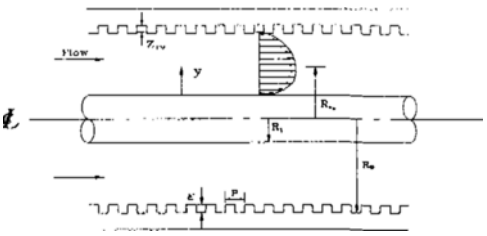

(c) Case

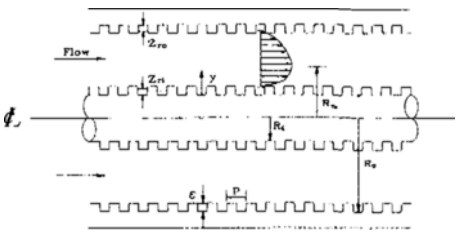

(d) Case

Fig. 1 Idealized model.

strongly affect the velocity and turbulence distributions. Moreover, for the evaluation of his results, Brighton assumed that the position of zero shear stress and of maximum velocity coincided, which has been proved to be untrue (Lawn & Elliott, 1971). Satake & Kawamura (1993) analyzed theoretically Rehme's results concerning the asymmetric turbulent flow in the annuli with small radius ratios. In contrast to the large number of experimental results on the flow in smooth concentric annuli mentioned above, only a few studies (Durst, 1968, Kim, 1994) have been published about the turbulent fluid flow characteristics in the roughened annuli. From these limited measurements, no conclusions can be drawn about the turbulent flow characteristics depending on the position of roughness in annuli. However, it is important to have detailed knowledge of the turbulent flow characteristics turbulence depending on the position of roughness as shown in Fig. 1. This is necessary to decide whether there are major deviations from the results of smooth annuli. Therefore, the present work can provide the basic data of theoretical analysis for the optimum roughness structure of the thermal industrial system.

2. Experimental Study

The experimental program undertaken by the present study is designed to check out the velocity profiles, friction factor, turbulence intensities, turbulent shear stresses, and turbulent kinetic energy. The working fluid is chosen as air in atmospheric conditions due to purposes of economical construction of test facilities and also availability of information on physical properties. The static pressure measurements are made with a MKS pressure transducer and the calibration of which is checked against a micro-manometer (FCO-12) at frequent intervals. Velocities are measured with a single Pitot tube and a X-type hot wire anemometer, and zero shear stress positions are measured from the u-v correlation coefficients with a X-type hot wire anemometer at radius ratios (α=0.26, 0.39, and 0.56), respectively. The total dimension of the main apparatus is about 6.1 meter in length. Air is drawn through a flow measuring orifice into an air filter and then through a bell-mouthed contraction section into the test section by a blower (0.8 kW, 3400 RPM) located at the extreme downstream end. The bell-mouthed section (minimum inner diameter, 97mm; maximum inner diameter, 160mm) is made from cast iron and the blower fan is rated 9 cubic m/min at 520 mmAq. The annular test

Table 1 Essential dimensionsl unit: mm.

		O.D.	I.D.	Material	$\alpha=(R_i/R_o)$	$De=2(R_o-R_i)$
Case(a)	Outer tube	113	97	Copper	0.26, 0.39, and 0.56	71.8, 58.4, and 43
	Core tube	25, 38, 54	23, 36, 52	Copper		
Case(b)	Outer tube	113	97	Copper		
	Core tube	25, 38, 54	22, 35, 51	Acryl		
Case(c)	Outer tube	117	97	Al-alloy		
	Core tube	25, 38, 54	23, 36, 52	Copper		
Case(d)	Outer tube	117	97	Al-alloy		
	Core tube	25, 38, 54	22, 35, 51	Acryl		

section consists of core tubes having three different outer diameters and outer tubes having 97 mm inner diameter as in Table 1. A specially designed traversing mechanism carries the measuring instrument.

With this mechanism, the relative radial displacement of a probe is measured within 0.025 mm by electrical contact. The core tubes are supported at three locations by 3-point carriers which allow for radial adjustments of the core tube. When the test sections are assembled and aligned, the concentricity of the core to the outer tube is checked. The eccentricity due to the lack of straightness of the tubes is negligible in most cases, but a maximum of 2% is noted. The taps for measuring the static pressure is designed specifically to minimize potential errors due to local pressure variation. The orifice of the flow rate measurement is calibrated by the numerical integration of the velocity profiles measured at test sections. The range of Reynolds number covered is from 15,000 to 66,000 approximately. The pressure and temperature of the ambient are also recorded before each run. All the measurements are carried out only late in the night to avoid disturbances on the main power supply. The main experimental variables for the present study are the radius ratio (α), and the ratio of distance between inner and outer tube to roughness height ($(R_o-R_i)/\varepsilon$), for roughness pitch to height ($P/\varepsilon=2$) as in Fig. 1. Two constant temperature anemometers (C.T.A., TSI Model 1054 A) with an X-type hotwire probe and a universal waveform analyzer (D-6000 Model 611, Data Precision Inc.) are used and the calibration is done with the Pitot tube of 4 mm in diameter and 350 mm in length and digital micro-manometer (Model FCO-12). The outputs from C.T.A. Bridge that are prevented from aliazing by passing through 5 kHz low-pass filter are simultaneously sampled as digital values by means of 14-bit A/D converter equiped in the universal waveform analyzer, and then are recorded at the diskettes through Data Recorder, with a sampling rate of 10,000 units per second corresponding to Niquist sample period.

3. Results and Discussion

3.1 Wall shear stresses

The fully developed flow regime could be determined from the pressure drops against the channel distance from the entrance and the mean velocity profile. The region 1.28m away from the entrance of channel could be considered as the fully developed one for all cases of radius ratios.

$$\tau=\frac{dp}{dx}\left(\frac{r^2-R_{\tau_0}{}^2}{2}\right)\frac{1}{r},\quad R_{\tau_0}\le r\le R_o \tag{1}$$

$$\tau=-\frac{dp}{dx}\left(\frac{R_{\tau_0}{}^2-r^2}{2}\right)\frac{1}{r},\quad R_i\le r\le R_{\tau_0} \tag{2}$$

where $R_{\tau 0}$ is the position of zero shear stress (see Fig. 1). Substituting the measured dp/dx and zero shear stress position into Eqs. (1) and (2), the wall shear stresses, τ_{wo} and τ_{wi} on the core and outer walls are respectively obtained. Figure 2 shows as an example of case (b) that the inner

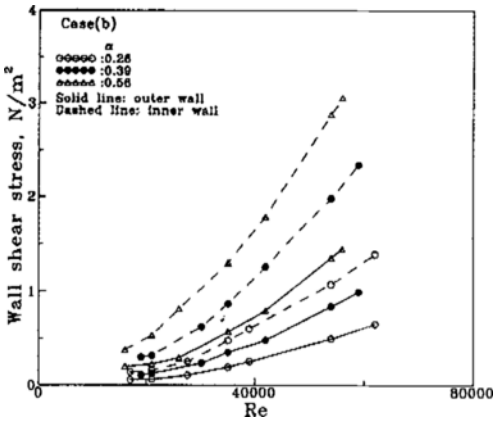

Fig. 2 Wall shear stresses against Re.

and outer wall shear stresses are the functions of radius ratios and Reynolds numbers. The larger the radius ratio (α) becomes, the more the shear stress increases, which seems to be attributed from the phenomenon that the higher bulk velocity generates at the narrower clearance between the inner and the outer tubes at the same Reynolds number. A noteworthy feature of the data for four cases is that the difference between the inner and the outer wall shear stresses is strongly dependent upon the radius ratio (α) and the position of roughness on the wall, thus, it is expected that the condition of equality of τ_{wo} and τ_{wi} may be able to happen at a certain radius ratio (α). It is the reason that the shear stress distribution of Eqs. (1) and (2) is subject to the position of zero shear stress.

3.2 Mean velocity distribution

The time mean velocity profiles are measured with a X-type hot wire probe at four different cases in the position 3.75 m away from the channel entrance. Figure 3 shows the dimensionless time mean velocities at α=0.39 and Re=54,000, at which one can observe the processes of velocity distributions depending on the position of roughness. Open circular symbols obtained from the smooth annuli of case (a) are included as a reference to check up the effect of roughness position. The values in the case (a) are very good agreement with results of Park (1971) except for the region close to the wall. Figure 3 shows that the velocity distributions are strongly influenced

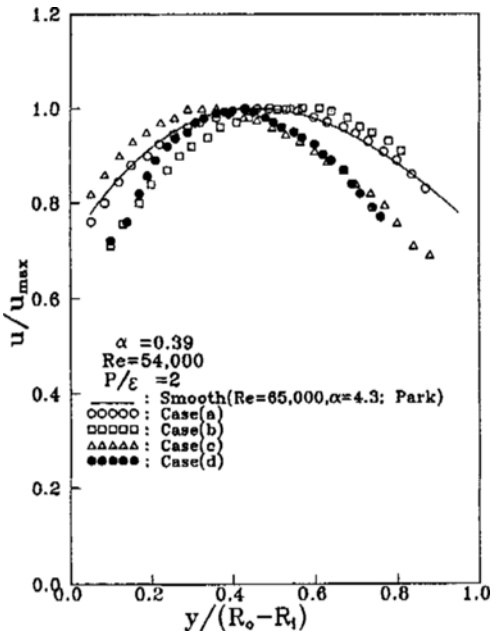

Fig. 3 Velocity distribution.

by the roughness position of annuli. It is also recognized that the velocity distributions closer to the rough wall are developed in a slower slant because the square-ribbed roughness on the wall hinders the axial fluid flow. The case (c) has the most asymmetric contour. It is because the roughness on the outer wall affects the static pressure drop relating to the velocity profile more strongly than that of the inner tube. The dimensionless mean velocity distributions are almost same regardless of Reynolds numbers ranging from 20,000 to 60,000.

3.3 Friction factor

Using each wall shear stress, τ_{wo} and τ_{wi} obtained from Eqs. (1) and (2), the inner and the outer wall friction factors, f_i and f_o can be given by:

$$f_i=\frac{\tau_{wi}}{0.5\rho u_b^2} \tag{3}$$

$$f_o=\frac{\tau_{wo}}{0.5\rho u_b^2} \tag{4}$$

where ρ and u_b are the air density and the bulk velocity, respectively. And the averaged friction factor f is defined as:

$$f=\frac{R_o f_o+R_i f_i}{R_o+R_i} \tag{5}$$

Figure 4 compares the friction factors depending on the radius ratio(α) and the position of roughness shown in Fig. 1. The present results indicate that the case (d) results in the highest friction factor enhancement, followed by the case (c), the case (b), and the case (a), respectively. It is supposed to be attributed from the differential influence of fluid flow in an accordance with the position of roughness elements. The measured values for the smooth annuli, case (a) lie in good agreement with Park's data (1971). Park's data for smooth annuli indicate that the friction factors are higher at a lower radius ratio having wide duct; however, considering the measured variation of radius ratio (α) at the case (d), the most striking feature of the diagram shows that the friction factors are not evenly higher with the lower radius ratio (α); that is, the values for $\alpha=$ 0.39 become highest. It is the reason that, though the friction factors are subject to bulk velocity shown in Eqs. (3) and (4), the values are in fact shown as a function of Reynolds number ($Re=u_b De/\nu$) in Fig. 4, at which u_b and De mean the bulk velocity and the equivalent diameter, respectively. Because the bulk velocity is dependent upon the radius ratio (α) at the constant Re, it is believed that the correlation of α and the friction factor may be able to be functionable.

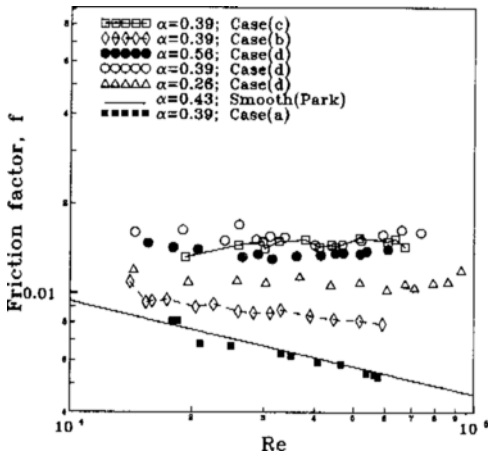

Fig. 4 Friction factor.

3.4 Turbulence intensity

The three directional (u, v, and w) turbulent intensities measured are plotted in Figs. 5-7, for three Reynolds numbers and three radius ratios against dimensionless radial distance normal to the inner wall. Each figure shows the turbulence intensities for three different radius ratios (α) of 0.26, 0.39 and 0.56, at which the intensities shown as dashed lines at cases (a), (b), (c) and rectangular soild symbols at $\alpha=0.26$ and 0.39 of case (d) represent the averaged values over three different Reynolds numbers. The turbulence intensities measured are made dimensionless by the friction velocities of the outer wall ($u_{\tau o}=\sqrt{\frac{\tau_{wo}}{\rho}}$) which are deduced from the force balance and the position of zero shear stress measured by the X-type hot wire anemometer. The turbulence intensities measured in the smooth annuli of $\alpha=$ 0.56 by Brighton and Jones (1964) are included in the diagrams as solid lines. The results are reasonably in line with those of present studies

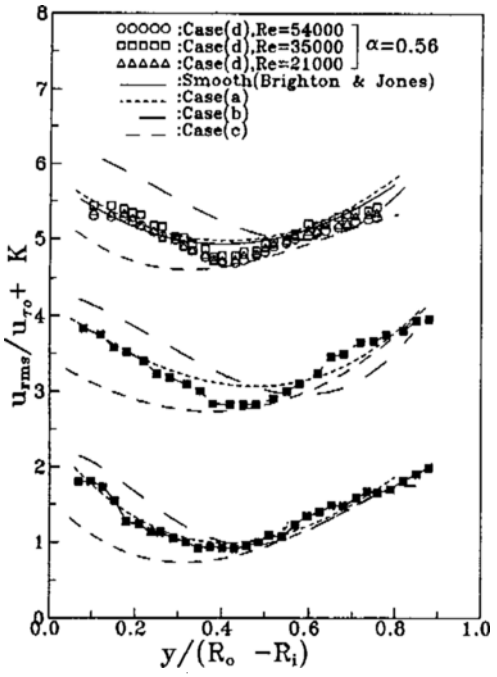

Fig. 5 Experimental results for axial turbulence intensity against dimensionless distance from the inner wall: $\alpha=0.26$(K=0); $\alpha=0.39$(K=2); $\alpha=0.56$(K=4). Solid line, Brighton & Jones' results (1964) of smooth annulus.

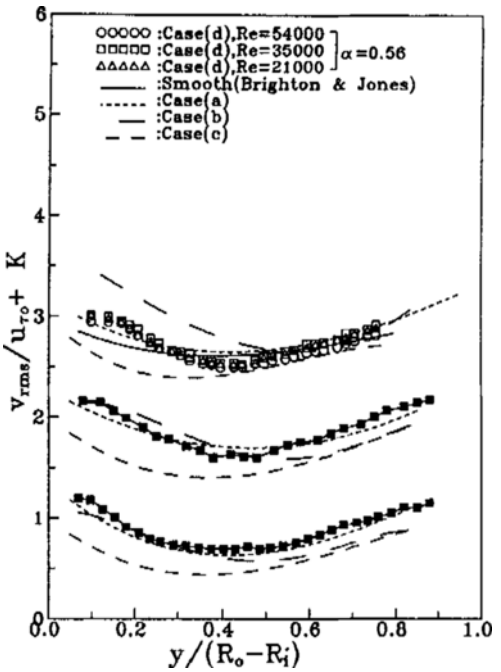

Fig. 6 Experimental results for radial turbulence intensity against dimensionless distance from the inner wall: $\alpha=0.26$(K=0); $\alpha=0.39$(K=1); $\alpha=0.56$(K=2), other symbols as in Fig. 5.

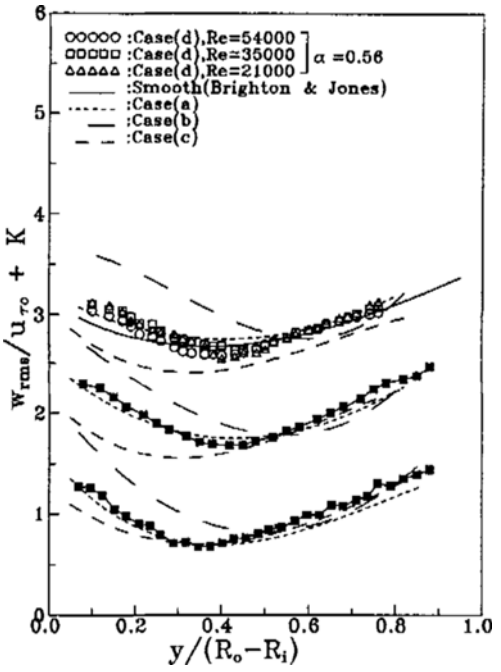

Fig. 7 Experimental results for azimuthal turbulence intensity against dimensionless distance from the inner wall: symbols as in Fig. 6.

for three (u, v, w) directions.

For the smaller radius ratios (α) of cases (a) and (d), the intensity distributions have more asymmetric tendency because the difference of turbulent kinetic energy and the fluid element size between the region close to core tube and the region close to outer tube is higher. With increasing a radius ratio, the turbulence intensities of case (d) in the axial (u) direction are slightly lower than those of smooth annuli around the position of zero shear stress for the cases of $\alpha=0.39$ and 0.56, but almost same for the case of $\alpha=0.26$. The dimensionless axial intensities ($u_{rms}/u_{\tau 0}$) of case (d) for the radius ratio (α) =0.56 are much smaller than those in the case (b) in the neighbourhood of core tube but almost same at the region close to the outer wall because the more friction loss by roughness effect is generated at the narrower distance between inner and outer tubes.

Observing all the intensity distributions, the portion having minimum intensities gradually moves to the inner side with decreasing the radius ratio (α), it is because the annular tube in geometry becomes gradually closer to the circular tube with decrease of the radius ratio(α). The turbulence intensities in the radial (v) direction are usually smaller than those of the axial(u) direction and the intensity distributions close to the outer tube become generally in a lower slope rather than near the inner tube. The tendency that the scatterings of measured data become wider with decreasing radius ratio (α) is attributed to the relatively reduced roughness effect because of wider cross-section, which is true with the smooth annuli. The measured data show that the radial intensities of cases (b) and (d) are higher than those of cases (a) and (c) in the inner side, it seems that the turbulent fluctuating components are significantly influenced by the square-ribbed roughness.

As shown in Fig. 7, turbulence intensities in the azimuthal (w) direction usually having the similar axial intensities generally show the same behaviour as the values of circular tubes (Laufer, 1954).

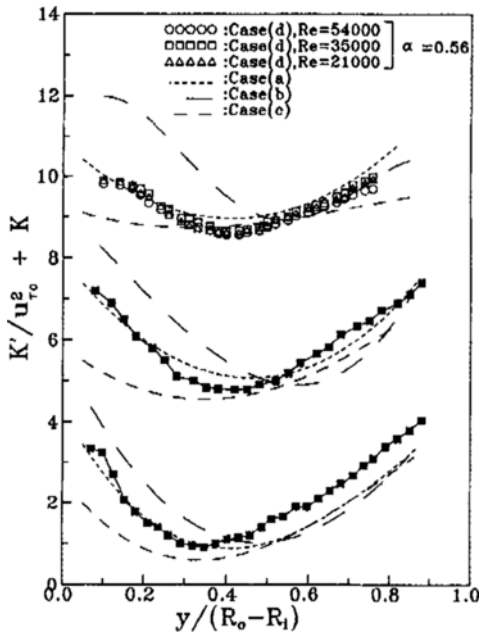

Fig. 8 Experimental results for kinetic energy of turbulence against dimensionless distance from the wall: $\alpha=0.26$(K=0); $\alpha=0.39$(K=4); $\alpha=0.56$(K=8). Other symbols as in Fig. 5.

3.5 Turbulent kinetic energy

The kinetic energy of turbulence can be calculated as the sum of the intensities in the three directions as follows:

$$\overline{k'}=0.5(\overline{u}'^2+\overline{v}'^2+\overline{w}'^2) \tag{6}$$

Figure 8 represents the calculated values divided by the square of the friction velocity on the outer wall. A noteworthy feature of Fig. 8 is that with increasing α like results of smooth annuli (Brighton & Jones, 1964), the turbulent kinetic energy of all cases except case (b) increases to be at the slower slant. For the case of $\alpha=0.56$ the kinetic energy distributions of cases (a), (c) and (d) become less steep, but the dimensionless distributions of case (b) become steeper because the frictional losses at the outer wall get relatively smaller. It seems probable that, for the radius ratio $\alpha=0.56$ with the narrower distance between the inner and outer tubes approaching the 2-dimensional channel, the whole flow field becomes significantly subject to roughness effect. Whereas, for the case of (d), the measured values of $\alpha=0.39$ at the region close to the outer wall are considerably lower than those of $\alpha=0.26$. This behaviour is expected that since the cross sectional areas in annuli become significantly wider, the kinetic energy depends on the structure of turbulence in terms of effects of roughness but less detectable influence of the velocity gradient on the outer wall.

4. Conclusions

This experimental study was done on the structure of turbulent flow in concentric annuli for four different cases of variations of radius ratio (α) and Reynolds number. The following conclusions are obtained from the comparison of smooth annular results:

(1) It is found in the time mean velocity distributions that the case (c) has the most asymmetric contour because the roughness on the outer wall affects the static pressure drop relating to a velocity profile more strongly than that of the inner tube.

(2) Though the friction factors for smooth annuli are higher at a lower radius ratio, the friction factors for the case (d) are not evenly higher with lower radius ratio (α); that is, the values for $\alpha=0.39$ become highest.

(3) It is indicated that the case (d) results in the highest friction factor enhancement, followed by the case (c), the case (b), and the case (a), respectively.

Reference

Brighton, J. B., 1963, "The Structure of Fully Developed Turbulent Flow in Annuli," *Ph. D. Thesis*, Purdue University.

Brighton, J. A. and Jones, J. B., 1964, "Fully-Developed Turbulent Flow in Annuli," *J. Basic Engng*, D86, p. 835.

Durst, F., 1968, *On Turbulent Flow through Annular Passages with Smooth and Rough Core*, M. Sc. Thesis, Imperial College.

Laufer, J., 1954, "The Structure of Turbulence in Fully Developed Pipe Flow," *N. A. C. A. Tech. Note*, No. 1174.

Lawn, C. J. and Elliott, C. J., 1971, "Fully Developed Turbulent Flow through Concentric Annuli," C. E. G. B., Rep. RD/B/N/1878.

Kim, K. C., Ahn, S. W. and Lee, B. G., 1994, "Turbulence Structures of Flow in Concentric Annuli with Rough Outer wall," *Journal of KSME*, Vol. 18, No. 9, pp. 2443~2453(in Korea).

Kjellstr m, B. and Hedburg, S., 1966, "On Shear Stress Distributions for Flow in Smooth or Partially Rough Annuli," AB Atomenergi, Studsvik, Rep. AE-243.

Park, S. D., 1971, "Developing Turbulent Flow in Concentric Annuli; An Analytical and Experimental Study," *Ph. D. Thesis, Dept. of Mech. Eng.*, University of Ottawa.

Rehme, K., 1974, "Turbulent Flow in Smooth Concentric Annuli with Small Radius Ratios," *J. Fluid Mech.* Vol. 64, p. 263.

Satake, S. I. and Kawamura, H. 1993, "Large Eddy Simulation of Turbulent Flow in Concentric Annuli with a Thin Inner Rod," *9th Symposium on "Turbulent Shear Flow"*, Kyoto, Japan, August, 5. 5. 1-5. 5. 6.